

RESEARCH ARTICLE

"This is the peer reviewed version of the following article: [Angew. Chem. Int. Ed. 2021, 60,3737 – 3744], which has been published in final form at [Link to final article using the DOI: doi.org/10.1002/anie.202013473]. This article may be used for non-commercial purposes in accordance with Wiley Terms and Conditions for Self-Archiving."

Delivery of a Masked Uranium(II) by an Oxide-Bridged Diuranium(III) Complex

Dieuwertje K. Modder,^[a] Chad T. Palumbo,^[a] Iskander Douair,^[b] Farzaneh Fadaei-Tirani,^[a] Laurent Maron,^[b] and Marinella Mazzanti*^[a]

[a] D. K. Modder, Dr. C. T. Palumbo, F. Fadaei-Tirani, Prof. M. Mazzanti
Institut des Sciences et Ingénierie Chimiques
Ecole Polytechnique Fédérale de Lausanne (EPFL)
1015 Lausanne (Switzerland)
E-mail: marinella.mazzanti@epfl.ch

[b] I. Douair, Prof. L. Maron
Laboratoire de Physique et Chimie des Nano-objets
Institut National des Sciences Appliquées
31077 Toulouse, Cedex 4 (France)

Supporting information for this article is given via a link at the end of the document.

Abstract: Oxide is an attractive linker for building polymetallic complexes that provide molecular models for metal oxides activity, but studies of these systems are limited to metals in high oxidation states. Herein, we synthesized and characterized the molecular and electronic structure of diuranium bridged U(III)/U(IV) and U(III)/U(III) complexes. Reactivity studies of these complexes revealed that the U–O bond is easily broken upon addition of N-heterocycles resulting in the delivery of a formal equivalent of U(III) and U(II), respectively, along with the uranium(IV) terminal-oxo coproduct. In particular, the U(III)/U(III) oxide complex effects the reductive coupling of pyridine and two-electron reduction of 4,4'-bipyridine affording unique examples of diuranium(III) complexes bridged by N-heterocyclic redox-active ligands. These results provide insight into the chemistry of low oxidation state metal oxides and demonstrate the use of oxo-bridged U(III)/U(III) complexes as a strategy to explore U(II) reactivity.

Introduction

Low oxidation state uranium compounds have shown high reactivity in the activation and functionalization of unreactive small molecules such as N₂, CO₂ and CO.^[1] However, the multi-electron transfer processes required for small molecule transformations are not common in uranium chemistry. Examples of single metal two- and three electron transfer^[1a, 2, 3] by U(III) complexes have been reported but remain scarce. Well defined molecular uranium(II) complexes have been recently isolated^[4] with different supporting ligands but their reactivity remains practically unexplored^[5] partly due to the difficulty in controlling the reactivity of such reducing species. Notably, a first study indicated that although U(II) complexes can effect two-electron transfer to cyclooctatetraene, the reactivity is less clean compared to the

Th(II) analogue due to the competitive one-electron transfer reaction producing stable U(III) species.^[5]

Alternatively, multi-electron transfer processes can be implemented by building polymetallic uranium complexes^[1a, 1c, 6] or by associating uranium to redox-active ligands.^[3a, 7] Notably, the first examples of nitride-bridged diuranium(III) complexes^[8] were recently prepared in our group using siloxide supporting ligands. These complexes are able to transfer four electrons to dinitrogen (two electrons from each metal center) affording a diuranium(V) complex of the (N₂)⁴⁻ ligand^[6] that could be further functionalized by protons or CO to afford ammonia and cyanate, respectively. However, examples of polymetallic complexes of low oxidation state uranium remain scarce due to the lack of rational methods for their synthesis.

Among the first few reported examples of low oxidation state diuranium complexes is the uranium arene (μ -C₇H₈)[U(N[R]Ar)₂]₂ that was shown by Diaconescu and coworkers to behave as a four-electron reductant, reactivity consistent with a formal uranium(II),^[7f] although the spectroscopic and computational analysis of the electronic structure point to the presence of a U(III)-toluene dianion.^[9] More recently, the same dinuclear complex was also shown to reduce 2,2'-bipyridine (2,2'-bpy) to afford U(IV) complexes of the 2,2'-bpy^{•-} radical anion,^[10] by effecting a four-electron transfer. This provided a rare example of bipyridine reduction by a uranium complex.

F-element complexes of reduced N-heterocycles have attracted attention for their ability to promote magnetic coupling between lanthanide centers,^[11] and their ability to store electrons that can become available for small molecule activation.^[12] Several examples of N-heterocycles reduction including pyridine and bipyridine have been reported in lanthanide(II)^[13, 14] and in thorium(III)^[15] chemistry. Uranium(III) complexes have been reported to promote the reductive coupling of polyazines such as pyrazine and 2,4,6-tris(2-pyridyl)-1,3,5-triazine,^[16] but reduction of

RESEARCH ARTICLE

pyridine, 2,2'-bipyridine (2,2'-bpy) and 4,4'-bipyridine (4,4'-bpy) was not observed for U(III) complexes supported by cyclopentadienyl or hydrotris(3,5-dimethylpyrazolyl) borate ligands.^[12c, 17] Direct reduction of bipyridine by a U(III) complex was only reported recently by Meyer and coworkers for the triaryloxide complex $[(\text{Ad}, \text{tBuArO})_3\text{tacn}]\text{U}$ complex.^[18] Examples of uranium complexes of bipyridine radicals^[10, 12a-c, 19] remain rare, and only two examples of uranium complexes of the diamagnetic bipy²⁻ ligand were reported.^[18, 20]

Oxide is an attractive linker group for building polymetallic complexes but the involved synthetic methods (oxo-transfer reaction to low oxidation state metal complexes) usually lead to metal complexes in high oxidation state. Notably, only a handful of rationally synthesised diuranium(IV) oxo-bridged complexes have been reported, probably due to the tendency of these species to undergo further oxidation.^[6, 21, 22] The first example of a crystallographically characterized U(III)–O–U(III) complex^[23] was isolated from solvent cleavage during the reduction of a U(III) complex, but only recently we reported the first reproducible synthesis of a U(III)–O–U(III) complex.^[6] Bridging oxides are usually inert and only one example of substitution reactivity at a bridging oxide has been reported so far in uranium chemistry.^[24] Cleavage of the thermally inert M–O–M fragment was reported to occur for Fe(III) to yield a reactive Fe(IV)=O and Fe(II) but only under photolytic conditions.^[25]

Here we describe the second example of a reproducible synthesis of an oxide-bridged diuranium(III) complex and report the reactivity of this complex and its U(III)–O–U(IV) analogue with N-heterocycles. We found that the oxide bridge is readily cleaved at low temperature to afford a U(IV) terminal oxo complex, while the electrons stored in the U(III)–O–U(IV) and U(III)–O–U(III) fragment are cleanly transferred to N-heterocycles. Remarkably the U(III)–O–U(III) complex acts as a “masked U(II)” in the reduction of pyridine, 2,2'-bpy, and 4,4'-bpy. The higher stability of the U(III)–O–U(III) complex compared to the isolated analogous U(II) species results in a more facile and controlled reactivity.

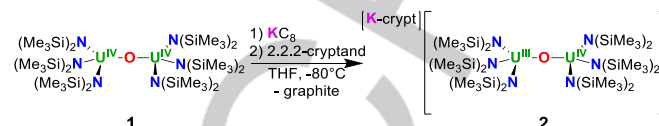
Results and Discussion

Synthesis of U(III)/U(IV) and U(III)/U(III) Oxide Complexes.

In view of the attractive reactivity demonstrated by the siloxide supported U(III)–O–U(III) complex $[(\text{K}_2[\text{U}(\text{OSi}(\text{O}^t\text{Bu})_3]_2(\mu\text{-O}))]$,^[6] we decided to explore the possibility of accessing diuranium(III) oxides using different supporting ligands. We have chosen to investigate the $(\text{Me}_3\text{Si})_2\text{N}$ supporting ligand because a synthetic procedure for the synthesis of the amide supported U(IV)–O–U(IV) had been reported.^[22c]

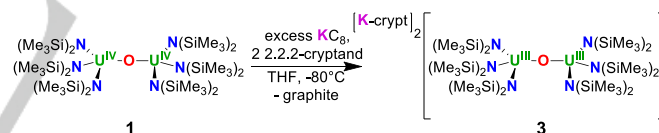
The previously reported^[22c] complex $[(\text{Me}_3\text{Si})_2\text{N})_3\text{U}_2(\mu\text{-O})]$, **1** was prepared in 68% yield using a modified procedure that uses the N-heterocyclic carbene 1,3-dimesitylimidazol-2-ylidene (IMesN_2O)^[6] as an oxygen atom transfer reagent in the oxidation of $[\text{U}(\text{N}(\text{SiMe}_3)_2)]$ (see Supplementary Information). Complex **1** reacts with one equivalent of KC_8 at -80°C to yield a new complex with six ¹H NMR signals at low temperature, of which two

partially overlap (see Figures S2–S3 for variable temperature NMR data). Addition of 2.2.2-cryptand to the purple mixture did not shift the signals but facilitated crystallization after diffusion of hexane into the solution; crystals were obtained in 74% yield (Scheme 1) and were not obtainable in the absence of 2.2.2-cryptand. The crystals were identified by single crystal X-ray crystallography as the oxo bridged U(III)/U(IV) complex $[\text{K}(\text{2.2.2-cryptand})]_2[(\text{Me}_3\text{Si})_2\text{N})_3\text{U}_2(\mu\text{-O})]$, **2**.



Scheme 1. Reduction of **1**, with 1 eq KC_8 to yield **2**.

When **1** was reacted with excess KC_8 in the presence of 2.2.2-cryptand (2 equiv.) at -80°C in THF, the color of the solution changed to purple, and one new set of signals was observed in the ¹H NMR spectrum (Figure S4). Diffusion of Et_2O into a concentrated THF solution of the reaction mixture at -40°C gave single-crystals in 70% yield of $[\text{K}(\text{2.2.2-cryptand})]_2[(\text{Me}_3\text{Si})_2\text{N})_3\text{U}_2(\mu\text{-O})]$, **3** (Scheme 2), characterized by X-ray crystallography. Complex **3** is insoluble in toluene, slightly soluble in Et_2O , and completely soluble in THF. Complex **3** is temperature sensitive and decomposes in solution above 0°C to afford multiple products including $[\text{K}(\text{2.2.2-cryptand})][\text{N}(\text{SiMe}_3)_2]$, $[\text{K}(\text{2.2.2-cryptand})][\text{U}(\text{N}(\text{SiMe}_3)_2)_4]$ and $[\text{K}(\text{2.2.2-cryptand})][(\text{Me}_3\text{Si})_2\text{N})_3\text{U}(\text{O})]$ (Figure S5). After 10 minutes at room temperature, approximately 70% of **3** remains. About 20% remains after 2 days at room temperature, and after 1 week **3** could no longer be observed.



Scheme 2. Reduction of **1**, with excess KC_8 to yield **3**

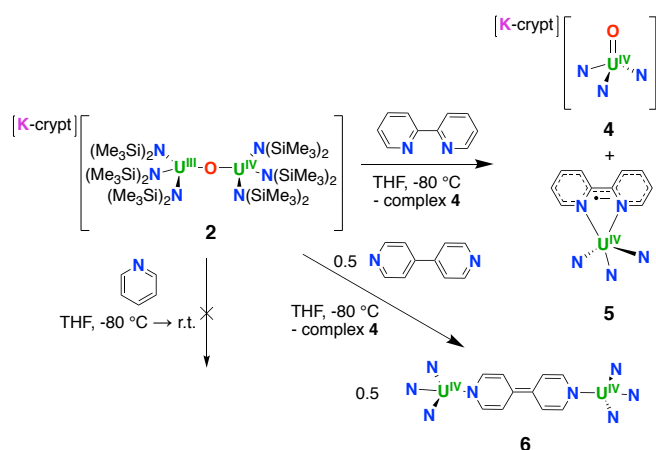
The molecular structures of **2** and **3** consist of monoanionic and dianionic oxide bridged dinuclear U(III)/U(IV) and U(III)/U(III) complexes and one and two $[\text{K}(\text{2.2.2-cryptand})]^+$ cations respectively (See infra).

Reactivity of oxide complexes

Reactivity studies of the two low oxidation state uranium oxide complexes **2** and **3** with aromatic heterocycles revealed that one of the U–O bonds is readily cleaved at low temperature delivering a formal equivalent of U(III) and U(II), respectively, and the U(IV) oxo coproduct, $[\text{K}(\text{2.2.2-cryptand})][(\text{Me}_3\text{Si})_2\text{N})_3\text{U}(\text{O})]$, **4**. To unambiguously confirm the formation of complex **4** in these reactions, we also prepared it using an independent route. The reduction of the previously reported U(V) analogue $[(\text{Me}_3\text{Si})_2\text{N})_3\text{U}(\text{O})]$ with KC_8 in the presence of cryptand (see the Supplementary Information) afforded complex **4** in 62% yield. The solid-state structure of complex **4** was determined by crystallography and is reported in the supporting information (Figure S28). The reactivity of **2** and **3** is summarized in Schemes 3 and 4, respectively.

RESEARCH ARTICLE

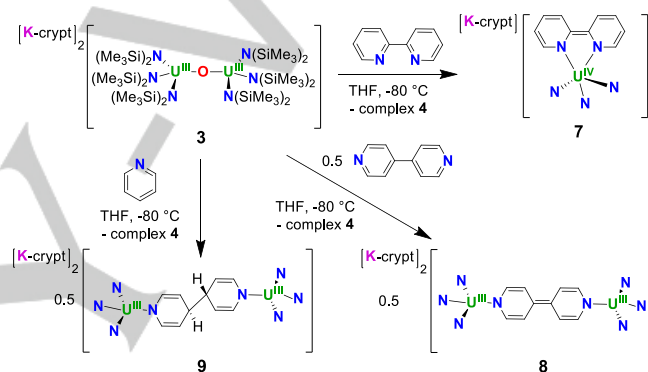
Complex **2** reacts with 2,2'-bpy and 4,4'-bpy to yield the U(IV) products $[(\text{Me}_3\text{Si})_2\text{N})_3\text{U}(2,2'\text{-bpy}^{\cdot-})]$, **5**, and $[\{(\text{Me}_3\text{Si})_2\text{N})_3\text{U}\}_2\{\mu\text{-(4,4'-bpy}^{2-})\}]$, **6**, respectively, along with **4** (Scheme 3). Reactivity with pyridine was not observed. Pyridine reduction by a uranium complex was not reported previously and this is explained in terms of the low redox potential of pyridine ($E_{1/2}$ in DMF vs. Ag/AgCl: py = -2.76 V; 2,2' bpy = -2.19 and -2.76 V; 4,4'-bpy = -1.91 and -2.47 V).^[26]



Scheme 3. Reaction of **2**, with 2,2'-bipyridine to yield **5**, and with 4,4'-bipyridine to yield **6**.

When a THF- d_8 solution of 2,2'-bpy was added to dark purple crystals of **2** at -80 °C, the color immediately changed to green and yielded complex **5**. The measured metrical parameters are consistent with the presence of a monometallic U(IV) complex, containing a 2,2'-bipyridinyl radical anion. In contrast, the reaction of **2** with 4,4'-bpy resulted in the two-electron reduction of the bipyridine and the formation of a (4,4'-bipyridinyl) $^{2-}$ bridged diuranium(IV) complex. The solid-state structure of **6** shows a bimetallic uranium(IV) complex and X-ray data fully support the U(IV)/(4,4'-bipyridinyl) $^{2-}$ charge assignment. The observed reactivity of **2** with 2,2'-bpy and 4,4'-bpy can be interpreted in terms of cleavage of the U(III)–O–U(IV) bond induced by the binding of the bpy ligands resulting in the release of the U(IV) terminal oxo complex **4**. Concomitant reduction of the bipyridines by the $(\text{Me}_3\text{Si})_2\text{N})_3\text{U(III)}$ synthon leads to the complexes **5** and **6**. This interpretation was corroborated by DFT studies (see *infra*) and by the reactivity of $[\text{U}(\text{N}(\text{SiMe}_3)_2)_3]$. Notably, independent studies showed that $[\text{U}(\text{N}(\text{SiMe}_3)_2)_3]$ reacts analogously to **2**; the reactions of $[\text{U}(\text{N}(\text{SiMe}_3)_2)_3]$ with 2,2'-bpy and 4,4'-bpy also yielded complexes **5** and **6** in 56% and 69% yield, respectively, providing a rare example of direct reduction of bipyridine by a U(III) complex (see Supplementary Information for details). Complex **6** reacted readily with two equiv. of $^{13}\text{CO}_2$ releasing 4,4'-bpy. Evaporation of the resulting mixture and quenching with D_2O showed the quantitative formation of $^{13}\text{CO}_3^{2-}$ by quantitative $^{13}\text{C}\{^1\text{H}\}$ NMR spectroscopy. This result demonstrates that the two electrons stored in the reduced bipyridine are used to effect the reductive disproportionation of CO_2 to quantitatively yield carbonate and CO (see supporting information).

A remarkable behavior was observed for **3** during the reductive reactions of N-heterocycles, which did not lead to the formation of dinuclear U(IV) complexes of reduced N-heterocycles as could have been anticipated. Instead, complex **3** was found to release, upon addition of pyridine, 2,2'-bpy, or 4,4'-bpy, the U(IV) oxo complex **4** and a “masked U(II)” that effected pyridine reductive coupling or double reduction of 2,2'-bpy and 4,4'-bpy (Scheme 4). Notably, the reaction of complex **3** with 2,2'-bpy and 4,4'-bpy gave bipyridinyl reduction products, namely $[\text{K}(2.2.2\text{-cryptand})][\{(\text{Me}_3\text{Si})_2\text{N})_3\text{U}(2,2'\text{-bpy})\}]$, **7**, and $[\text{K}(2.2.2\text{-cryptand})]_2[\{(\text{Me}_3\text{Si})_2\text{N})_3\text{U}\}_2\{\mu\text{-(4,4'-bpy)}\}]$, **8**. Moreover, in contrast to **2**, complex **3** also reacts with pyridine, forming the dinuclear uranium(III) complex bridged by a dianionic reductively coupled pyridinyl moiety, $[\text{K}(2.2.2\text{-cryptand})]_2[\{(\text{Me}_3\text{Si})_2\text{N})_3\text{U}\}_2\{\mu\text{-(pyr)}_2\}]$, **9**. Complexes **8** and **9** provide the first examples of diuranium(III) complexes bridged by N-heterocyclic redox-active ligands.



Scheme 4. Reaction of **3**, with 2,2'-bipyridine to yield **7**, and with 4,4'-bipyridine to yield **8**, and with pyridine to yield **9**.

Addition of a colorless solution of 2,2'-bpy in THF to dark purple crystals of **3** at -80 °C caused an immediate color change to dark gray, and resonances corresponding to the oxo complex **4** were observed in the ^1H NMR spectrum at -80 °C. In the room temperature ^1H NMR spectrum, an additional broad signal was observed at -9.0 ppm which was assigned to complex **7**. The X-ray measured structural parameters of **7** are consistent with the presence of an anionic U(IV) complex bound to a (2,2'-bpy) $^{2-}$ ligand.

The reaction of **3** with 4,4'-bpy in THF- d_8 at -80 °C led to an immediate color change from purple to dark brown, and the ^1H NMR spectrum showed new resonances at -5.7 and -20.3 ppm assigned to complex **8**, as well as resonances corresponding to complex **4**. The solid-state structure of complex **8** is similar to **6** but features two U(III) complexes bridged by a (4,4'-bpy) $^{2-}$ ligand instead of the two U(IV) found in **6**.

Pyridine reductive coupling by metal complexes is more rarely observed than bipyridine reduction.^[27] Examples of pyridine reduction by Sc-arene complexes,^[28] samarium(II),^[13a] thulium(II),^[14] and thorium(III)^[15] have been reported, but no examples of pyridine reduction by uranium complexes are known. Interestingly, complex **3** is able to reduce pyridine, making it the first U(III) complex able to effect this type of reactivity.

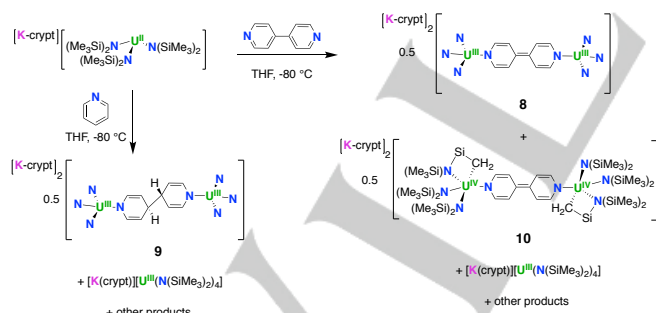
Upon addition of excess pyridine to a dark purple solution of complex **3** in THF- d_8 at -80 °C, new resonances at -6.7 and

RESEARCH ARTICLE

−20.8 ppm assigned to complex **9** were observed in the ^1H NMR spectrum at -80°C , as well as resonances corresponding to complex **4**. Diffusion of hexane into a THF solution of yielded a mixture of purple and pink crystals. Complex **9** can be separated from **4** by washing the solid with toluene and is stable in THF solution at room temperature for at least 48 hours. The solid-state structure of **9** shows a dianionic U(III)/U(III) complex where the two U(III) centers are bridged by two reductively coupled pyridine molecules, acting as a $(\text{pyridine}_2)^{2-}$ ligand.

We have also shown in this work that the $[\text{U}(\text{N}(\text{SiMe}_3)_2)_3]$ complex and complex **2** do not reduce pyridine, probably due to the high reducing power required to overcome the low reduction potential of pyridine ($E_{1/2}$ vs. Ag/AgCl : $\text{py} = -2.76\text{ V}$). Therefore, the reductive coupling of pyridine effected by complex **3** provides a unique access route to complex **9**. The formation of **9** can be interpreted in terms of the pyridine induced release of a U(II) synthon concomitant with formation of the complex **4**. This interpretation was corroborated by DFT calculations (see *infra*).

Since the synthesis of the U(II) complex $[\text{K}(2.2.2\text{-cryptand})][\text{U}^{\text{II}}(\text{N}(\text{SiMe}_3)_2)_3]$ was recently reported by Evans and coworkers,^[4d] we also explored the reaction of $[\text{K}(2.2.2\text{-cryptand})][\text{U}^{\text{II}}(\text{N}(\text{SiMe}_3)_2)_3]$ with N-heterocycles for comparison. Such a reaction was performed by generating and reacting the complex in situ at -80°C . Treatment of in situ generated solutions of $[\text{K}(2.2.2\text{-cryptand})][\text{U}(\text{N}(\text{SiMe}_3)_2)_3]$ with 4,4'-bpy and pyridine at -80°C produced **8** and **9**, respectively, which were observed by ^1H NMR spectroscopy (see Supplementary Information) and the latter also by X-ray crystallography. However, multiple products were formed in both reactions when the solution of $[\text{K}(2.2.2\text{-cryptand})][\text{U}(\text{N}(\text{SiMe}_3)_2)_3]$ prepared in situ was not used immediately (Scheme 5). Crystals of the U(IV) cyclometalate complex $[\text{K}(2.2.2\text{-cryptand})]_2[(\text{Me}_3\text{Si})_2\text{N})_2(\kappa^2\text{-C}_6\text{H}_4\text{SiMe}_2\text{NSiMe}_3)_2\text{U}]_2(4,4'\text{-bpy})$, **10**, were also isolated from the reaction of $[\text{K}(2.2.2\text{-cryptand})][\text{U}(\text{N}(\text{SiMe}_3)_2)_3]$ with 4,4'-bpy. These results confirm that the U(III)/U(III) oxide displays the same reactivity as a U(II) complex. However, the U(II) reactivity is more complicated to control than that of **3** and produces other unidentified products along with the cyclometalated U(IV) species **10**.



Scheme 5. Reaction of $[\text{K}(2.2.2\text{-cryptand})]_2[\text{U}(\text{N}(\text{SiMe}_3)_2)_3]$ with pyridine to yield **9** and other products and with 4,4'-bipyridine to yield complex **8**, variable amounts of **10** and other products.

Solid-State Structures

The structures of **2** (Figure S27) and **3** (Figure 1) show the presence of monoanionic and dianionic oxide bridged dinuclear uranium complexes in which each uranium center is four-coordinate and bound by three $\text{N}(\text{SiMe}_3)_2$ ligands and one bridging oxide ligand in a pseudo tetrahedral environment. These

structures are similar to the previously reported molecular structure of the neutral U(IV)/U(IV) dinuclear complex **1**.^[22c]

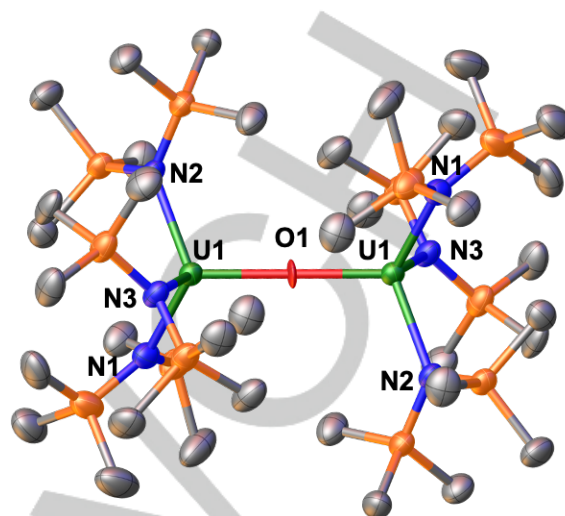


Figure 1. Molecular structure of the $[\{(\text{Me}_3\text{Si})_2\text{N}\}_3\text{U}_2(\mu\text{-O})]^{2-}$ anion in **3** with thermal ellipsoids drawn at the 50% probability level. Hydrogen atoms and the $[\text{K}(2.2.2\text{-cryptand})]$ counterions have been omitted for clarity.

The metrical parameters for complexes **1**, **2** and **3** are summarized in Table 1. All complexes exhibit nearly linear U–O–U angles and similar average N–U–O angles. However, there are differences in the U–O bond lengths. Complexes **1** and **3** both exhibit two equivalent or near-equivalent U–O bond lengths, but the U–O bonding in complex **2** is asymmetric (2.067(6) Å and 2.273(6) Å), suggesting localized bonding and charge distribution. Asymmetric bonding was also observed for the only other reported U(III)/U(IV) oxide-bridged complex, which is supported by a calix[4]tetrapyrrole ligand (U(III)–O_{oxo} 2.23(1) Å, U(IV)–O_{oxo} 2.02(1) Å).^[29] The U–O–U angle in **3** is significantly more linear compared to those found in the U(III)/U(III) cyclopentadienyl complex $[\{(\text{C}_5\text{Me}_5)_2\text{U}\}_2(\mu\text{-O})]^{2+}$ (171.5(6)°) or in the siloxide supported $[\text{K}_2\{\text{U}(\text{OSi}(\text{O}^t\text{Bu})_3)_3\}_2(\mu\text{-O})]^{6+}$ complex (where a potassium cation binds the oxide bridge). The U–N_{avg} bond distances increase as the oxidation state is decreased from 2.29(1) Å in **1** to 2.430(5) Å in **3**, as expected for reduction to U(III). The U...U distances of all three complexes are similar. Interestingly, the configuration of the ligands changes from nearly eclipsed in complexes **1** and **2** to staggered in complex **3**.

Table 1. Selected bond lengths (Å), angles (°), and torsion angles (°) of **1**, **2** and **3**.

Complex	1 [a]	2	3
U–O	2.142(6), 2.147(6)	2.067(6), 2.273(6)	2.159(2), 2.159(2)
U(IV)–N _{avg}	2.29(1)	2.335(6)	
U(III)–N _{avg}		2.381(6)	2.430(5)
U...U	4.2890(5)	4.3390(7)	4.3180(5)
U–O–U	179.2(4)	177.8(4)	180.0
N–U–O _{avg}	113(1)	112(1)	110(2)

RESEARCH ARTICLE

N–U–N_{avg}^[b] 14.8(8) 13.64(7) 60(1)

[a] data from ref ^[22c]. [b] Defined as the average angle between the two closest planes defined by N–U1–O and O–U2–N.

Single crystals of complex **5**, characterizable by X-ray crystallography could be grown by cooling a concentrated hexane solution of **5** to $-40\text{ }^{\circ}\text{C}$. The molecular structure of **5** (Figure 2) shows a neutral five-coordinate uranium complex supported by three N(SiMe₃)₂ ligands and one bidentate 2,2'-bpy ligand. In complexes containing reduced bipyridines, the C_{py}–C_{py} bond distance is the most revealing parameter in determining the charge on the bpy ligand. The C_{py}–C_{py} bond distance (C5–C6 = 1.416(4) Å) in **5** is similar to those found in other (2,2'-bipyridinyl)^{1–} complexes reported^[12a-c, 19] and consistent with the monoanionic charge assignment. For comparison, the C_{py}–C_{py} bond distance is 1.490(3) Å in free 2,2'-bpy,^[30] and 1.474 Å in the U(III) complex [(C₅Me₅)₂U(2,2-bpy)] with a neutral 2,2'-bpy.^[19c]

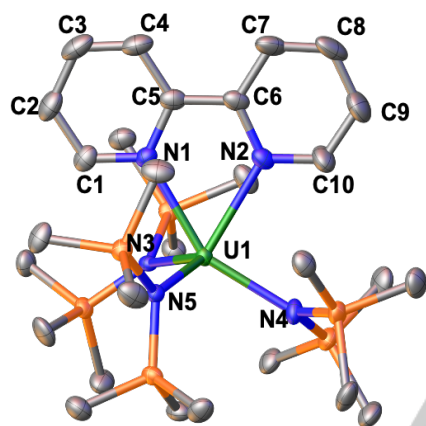


Figure 2. Molecular structure of **5**, with thermal ellipsoids drawn at the 50% probability level. Hydrogen atoms and disorder in the N(SiMe₃)₂ ligands have been omitted for clarity. Selected bond lengths (Å): U1–N1 2.464(2), U1–N2 2.464(2), C5–C6 1.416(4).

Single crystals of the diuranium(IV) product, **6**, characterizable by X-ray crystallography could be grown by cooling a concentrated hexane solution of **6** to $-40\text{ }^{\circ}\text{C}$. The complex (Figure 3) features two [(Me₃Si)₂N]₃U⁺ units bridged by a (4,4'-bpy)^{2–} ligand with the two uranium centers related by an inversion center. The U(IV) sites are four-coordinate in a distorted tetrahedral coordination environment, and the metrical parameters are consistent with this assignment. The range of U–N_{amide} bond distances (2.252(2)–2.283(2) Å) in **6** is typical of four-coordinate U(IV) amide complexes, e.g. [U(N(SiMe₃)₂)₄],^[31] and the U1–N1 bond distance of 2.278(2) Å is within this range, demonstrating the anionic nature of the bipyridinyl nitrogen. The value of the C_{py}–C_{py} bond distance of 1.380(5) Å in **6** is diagnostic of the inter-pyridyl double bond found in doubly reduced 4,4'-bpy.^[32] This value is similar to the value (1.376(10) Å) found in the Th(IV)/(4,4'-bipyridinyl)^{2–} complex [(C₅H₃(SiMe₃)₂)₃Th]₂[μ-(4,4'-bpy)] recently obtained from the reduction of 4,4'-bpy by a Th(III) complex.^[15] The C_{py}–C_{py} bond distance in **6** is also significantly shorter than the 1.47–1.48 Å range of C_{py}–C_{py} bond distances reported for An(IV) adducts of neutral 4,4'-bpy.^[17a, 33]

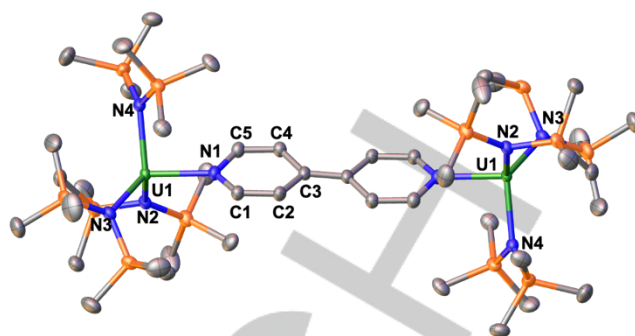


Figure 3. Molecular structure of **6**, with thermal ellipsoids drawn at the 50% probability level. Hydrogen have been omitted for clarity. Selected bond lengths (Å): U1–(N_{amide})_{avg} 2.264(14), U1–N1 2.278(2), C1–C2 1.356(3), C2–C3 1.458(4), C3–C3' 1.380(5), C3–C4 1.445(4), C4–C5 1.345(3).

Single crystals of **7** were grown by diffusion of hexane into the THF reaction mixture at $-40\text{ }^{\circ}\text{C}$. The structure of **7** (Figure S29) features a five-coordinate anionic (2,2'-bpy)^{2–}-uranium(IV) complex with a [K(2.2.2-cryptand)]⁺ counter cation. Notably, the contracted C_{py}–C_{py} bond of 1.369(8) Å in **7** compared to 1.416(4) Å in **5** suggests further ligand reduction to the 2,2'-bipyridinyl dianion. Accordingly, the U1–N1 and U1–N2 bonds shortened considerably from 2.464(2) Å in **5** to 2.335(4) Å and 2.386(4) Å in **7**. Moreover, the C_{py}–C_{py} bond distance is similar to those found in the previously reported actinide complexes of the 2,2'-bipyridinyl dianion (1.379(8) to 1.382(8) Å).^[18, 20, 34] Actinide complexes containing the 2,2'-bipyridinyl dianion are rare, with only three other examples reported to date, including the only example of a U(IV) / (2,2'-bpy)^{2–} complex, [K(2.2.2-cryptand)][((Ad₄tBuArO)₃tacn)U(2,2'-bpy)],^[18] the U(V) complex [Na(THF)₆][U(2,2'-bpy^{2–})₂(2,2'-bpy^{1–})₂],^[20] and a complex of thorium(IV), [(C₅Me₅)₂Th(2,2'-bpy)].^[34]

Single crystals of **8** were grown by hexane diffusion into the THF reaction mixture at $-40\text{ }^{\circ}\text{C}$. The solid-state structure of **8** (Figure S30) shows a bimetallic dianionic U(III)/U(III) complex with two [K(2.2.2-cryptand)]⁺ counter cations. The U(III) ions are four-coordinate and in a distorted tetrahedral coordination environment. The C_{py}–C_{py} bond distance of 1.393(8) Å in **8** is similar to the 1.380(5) Å distance in **6**, but the U1–(N_{amide})_{avg} bond length of 2.387(11) Å and the U1–N1 bond length of 2.402(4) Å are significantly longer compared to the U1–(N_{amide})_{avg} 2.264(14) Å and U–2.278(2) Å bond lengths in **6**. These metrical values indicate the presence of two U(III) ions and a dianionic 4,4'-bipyridyl ligand.

Single crystals of **9** were grown by hexane diffusion into the THF reaction mixture at $-40\text{ }^{\circ}\text{C}$. The solid-state structure of **9** (Figure 4) shows two [(Me₃Si)₂N]₃U(III)] units related by an inversion center with two [K(2.2.2-cryptand)]⁺ counter cations. The complex features two U(III) sites bridged by a (pyr₂)^{2–} ligand, and the U(III) ions are four-coordinate in a distorted tetrahedral coordination environment. The average U–N_{amide} bond distance of 2.385(5) Å and the U–N1 bond distance of 2.404(7) Å are similar to those observed in complex **8**, and in line with those of other four-coordinate U(III) complexes with anionic N-atom donors. In addition, the C_{py}–C_{py} bond distance of 1.570(17) Å is consistent with a single bond and close to the range of distances (1.559(4)–1.563(6) Å) reported for iron,^[35] samarium,^[13f] thulium,^[14] and thorium(III) complexes featuring reductively coupled pyridines.

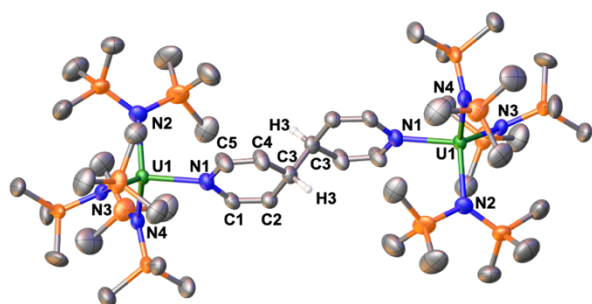


Figure 4. Molecular structure of the $[(\text{Me}_3\text{Si})_2\text{N})_2\text{U}_2\{\mu\text{-(pyr)}_2\}]^{2-}$ anion in **9** with thermal ellipsoids drawn at the 50% probability level. Hydrogen atoms, except for H3, and the $[\text{K}(2.2.2)\text{-cryptand}]^+$ counterions have been omitted for clarity. Selected bond lengths (Å): $\text{U1-(Namide)}_{\text{avg}}$ 2.385(5), U1-N1 2.404(7), C3-C3' 1.570(17).

The molecular structure of complex **10** shows the presence of the cyclometalate complex $[\text{K}(2.2.2\text{-cryptand})]_2[(\text{Me}_3\text{Si})_2\text{N})_2(\kappa^2\text{-C,N-CH}_2\text{SiMe}_2\text{NSiMe}_3)\text{U}_2(4,4'\text{-bpy})]$ (Figure S31) which consists of a dianionic dinuclear U(IV) complex and two $[\text{K}(2.2.2\text{-cryptand})]^+$ counter cations. The uranium centers are five-coordinated by two $\text{N}(\text{SiMe}_3)_2$ ligands, one bidentate $\text{N}(\text{SiMe}_3)(\text{SiMe}_2\text{CH}_2)$ ligand and a bridging $4,4'\text{-bpy}^{2-}$ ligand. The $\text{C}_{\text{py}}\text{-C}_{\text{py}}$ bond distance of 1.364(9) Å is similar to the one in complex **8** (1.393(8) Å), in line with a two-electron reduction of the $4,4'\text{-bpy}$ ligand. In addition, the $\text{U1-(Namide)}_{\text{avg}}$ distance of 2.307(6) Å is significantly shorter than in **8** (2.387(11) Å), which is in agreement with the U(IV) assignment.

Density Functional Theory Mechanism

In order to get more insight into the reaction of the uranium(III) containing oxide bridged complexes with pyridine and bipyridine, computational studies were carried out at the DFT level (B3PW91). Plausible reaction pathways (Figures 5 and 6) were determined for both complexes **2** and **3**.

The calculations suggest that the reaction of **3** with pyridine does not involve the formation of a pyridine adduct intermediate, as the coordination of the pyridine results in the breaking of one U–O bond as found at the transition state. The associated barrier is 28.3 kcal/mol in line with a kinetically accessible reaction. At the transition state, the pyridine is coordinating one uranium center, inducing the breaking of the U–O bond while forming the U–N_{pyridine} bond. This reaction is quite unusual since U–O–U complexes are usually inert. This reactivity can be explained by analyzing the bonding in the bimetallic oxo complex. The Molecular Orbitals (MO) diagram indicates the presence of three-center U–O–U bonds (see Figures S34–36) consisting of one sigma and two π bonds. Interestingly, the SOMO of the complex is a σ^* U–O–U interaction so that the σ interaction is strongly weakened. This explains the Wiberg Index (WBI) found (0.7) and is in line with some covalency in the U–O bonds. The latter is corroborated by the Natural Bonding Orbital (NBO) analysis that finds two strongly polarized U–O bonds (one per uranium center) toward O (92.5%) that are of π character (100% p orbital on O and 60% d/40% f on U).

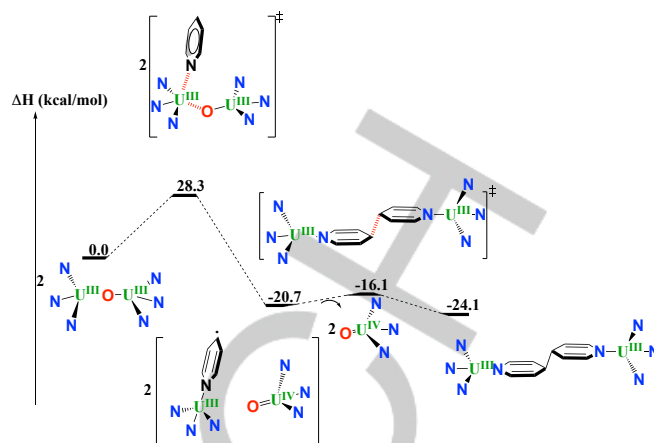


Figure 5. Computed enthalpy profile for the reaction of **3**, with pyridine.

Interestingly, the LUMO (see Figure S32) is an f orbital combination that is used to coordinate the pyridine lone pair. However, since the pyridine coordination is unsymmetrical (to only one U), this induces a second order Jahn Teller effect with a mixture between the SOMO, that is also an f combination with a U–O antibonding character, and the LUMO, allowing the U–O bond breaking as observed at the transition state. Following the intrinsic reaction coordinates, it yields the formation of a U(IV) terminal oxo complex and a U(III)(pyr[−]) complex that readily undergoes a radical coupling of two pyridines and yields complex **9** whose formation is strongly exothermic by 24.1 kcal/mol. The intermediate U(III)(pyr[−]) complex is unlikely to exist but computing the reaction in two steps renders the system computationally affordable. Therefore, the coordination of pyridine induces a formal disproportionation of the U(III)–O–U(III) complex into a U(IV) and a formal U(II) complex that reduces pyridine to afford the radical coupling of two pyridine rings. Radical coupling of two reduced pyridine rings was reported previously in low oxidation state lanthanide^[13f] and thorium^[15] chemistry.

The bonding of the mixed oxidation state U(III)/U(IV) oxide **2**, was investigated at the same level of theory. Quite interestingly, both molecular orbitals and NBO indicate the presence of the U(IV)=O bonds with very little interaction of the U(III). This is in line with the difference in calculated U–O bond distances (2.0 Å for the U(IV) vs. 2.4 Å for the U(III)–O) and further corroborated by the Wiberg bond indexes (1.4 for the U(IV)–O vs. 0.4 for the U(III)–O). The latter is smaller than what was found for complex **3**. Therefore, this mixed oxidation state oxide is better described as a U(III) adduct to the U(IV) terminal oxide complex. In addition, the reaction of **2** with 2,2'-bpy was computed. The reaction proceeds in the same way as **3** with pyridine (Figure 6). Despite the higher Lewis acidity of U(IV), the coordination of the bipyridine occurs at the U(III) center rather than the U(IV). This is mainly due to sterics as the U(IV)=O bond distance is shorter than the U(III)–O one. Even though the LUMO of the U(IV)–O–U(III) system only involves the U(IV)–O bonds, the LUMO+1, which is very close in energy, involves the U(III)–O interaction (Figure S37). Therefore, populating this LUMO+1 with the bipyridine nitrogen lone pairs will induce the breaking of the weak U(III)–O bond rather than the U(IV)–O one. The associated transition state was located, and the reaction barrier is 21.3 kcal/mol with respect to the separated reactants, which is kinetically accessible. Following the intrinsic reaction coordinates, it leads to the formation of the U(IV) terminal

RESEARCH ARTICLE

oxo complex, **4**, as observed in the reaction of **3** with pyridine, and the U(IV)(2,2'-bpy²⁻), **5**.

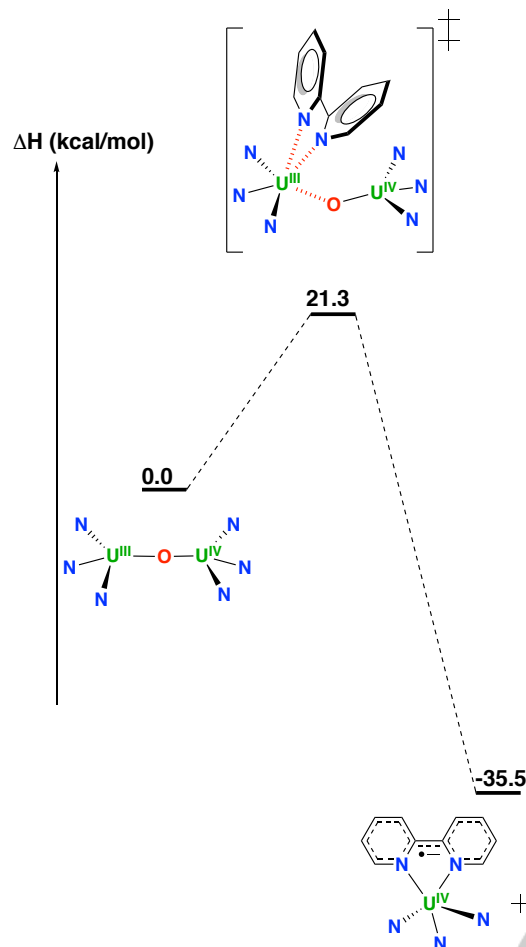


Figure 6. Computed enthalpy profile for the reaction of **2**, with 2,2'-bipyridine.

Conclusion

The N(SiMe₃)₂ ligand system allowed us to isolate the third example of an oxide bridged diuranium(III) complex and its U(III)/U(IV) analogue which were prepared by reduction of the U(IV)/U(IV) analogue. While the uranium oxide bonds are anticipated to be quite inert, we found that reduction of the metal center in oxide bridged complexes results in the weakening of the U(III)–O bonds. As a result, the addition of N-heterocycles to the oxide U(III)/U(IV) complex **2** leads to cleavage of one U–O bond and release of a “U(III)” synthon that reacts analogously to the mononuclear [U(N(SiMe₃)₂)₃] complex, providing a rare example of direct reduction of bipyridine by a U(III) complex. Surprisingly, the addition of N-heterocycles to the oxide U(III)/U(III) complex **3** led to the release of a “U(II)” synthon that effects the reduction of 4,4'-bpy and pyridine to yield the dinuclear U(III)/U(III) complexes bridged by a (4,4'-bpy)²⁻ and a dianionic reductively coupled pyridinyl moiety, respectively. The same compounds were also obtained from the reaction of the U(II) complex [K(2.2.2-cryptand)][U^{II}(N(SiMe₃)₂)₃] with pyridine or 4,4'-bpy, but other products, including cyclometalated side products, also formed. Therefore, the U(III)/U(III) oxide provides a tool for conveniently

exploring U(II)-like reactivity. Such reactivity allowed the synthesis of the first examples of dinuclear U(III)/U(III) complexes bridged by redox-active N-heterocyclic ligands.

Acknowledgements

We acknowledge support from the Swiss National Science Foundation grant number 200021_178793 and the Ecole Polytechnique Fédérale de Lausanne (EPFL). We thank Dr. Euro Solari for carrying out the elemental analyses, Rosario Scopelliti for important contributions to the X-ray single crystal structure analyses.

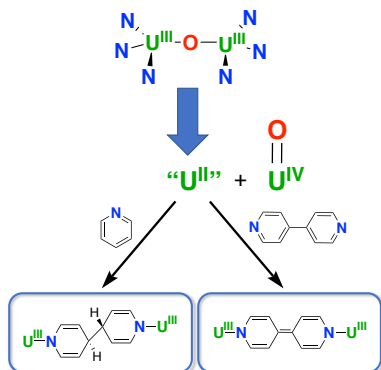
Keywords: uranium • polymetallic complexes • N-heterocycles • reduction • bipyridine

- [1] a) M. Falcone, L. Chatelain, R. Scopelliti, I. Zivkovic, M. Mazzanti, *Nature* **2017**, *547*, 332–335; b) P. L. Arnold, T. Ochiai, F. Y. T. Lam, R. P. Kelly, M. L. Seymour, L. Maron, *Nat. Chem.* **2020**, *12*, 654–659; c) L. Barluzzi, M. Falcone, M. Mazzanti, *Chem. Commun.* **2019**, *55*, 13031–13047; d) W. J. Evans, S. A. Kozimor, *Coord. Chem. Rev.* **2006**, *250*, 911–935; e) I. Castro-Rodriguez, K. Meyer, *Chem. Commun.* **2006**, 1353–1368; f) H. S. La Pierre, K. Meyer, in *Prog. Inorg. Chem.*, Vol. 58 (Ed.: K. D. Karlin), JOHN WILEY & SONS INC, HOBOKEN, **2014**, pp. 303–415; g) S. T. Liddle, *Angew. Chem. Int. Ed. Engl.* **2015**, *54*, 8604–8641; h) M. D. Walter, *Adv. Organomet. Chem.* **2016**, *65*, 261–377; i) P. L. Arnold, Z. R. Turner, *Nat. Rev. Chem.* **2017**, *1*; j) O. T. Summerscales, F. G. N. Cloke, in *Organometallic and Coordination Chemistry of the Actinides*, Vol. 127 (Ed.: T. E. Albrecht-Schmitt), **2008**, pp. 87–117; k) E. Barnea, M. S. Eisen, *Coord. Chem. Rev.* **2006**, *250*, 855–899; l) T. W. Hayton, *Chem. Commun.* **2013**, *49*, 2956–2973.
- [2] a) O. Cooper, C. Camp, J. Pécaut, C. E. Kefalidis, L. Maron, S. Gambarelli, M. Mazzanti, *J. Am. Chem. Soc.* **2014**, *136*, 6716–6723; b) D. M. King, F. Tuna, E. J. L. McInnes, J. McMaster, W. Lewis, A. J. Blake, S. T. Liddle, *Science* **2012**, *337*, 717–720; c) B. M. Gardner, C. E. Kefalidis, E. Lu, D. Patel, E. J. L. McInnes, F. Tuna, A. J. Wooles, L. Maron, S. T. Liddle, *Nat. Commun.* **2017**, *8*.
- [3] a) C. Camp, M. A. Antunes, G. Garcia, I. Ciofini, I. C. Santos, J. Pecaut, M. Almeida, J. Marcalo, M. Mazzanti, *Chem. Sci.* **2014**, *5*, 841–846; b) J. G. Brennan, R. A. Andersen, *J. Am. Chem. Soc.* **1985**, *107*, 514–516; c) D. S. J. Arney, C. J. Burns, *J. Am. Chem. Soc.* **1993**, *115*, 9840–9841; d) C. Camp, J. Pecaut, M. Mazzanti, *J. Am. Chem. Soc.* **2013**, *135*, 12101–12111; e) W. J. Evans, S. A. Kozimor, J. W. Ziller, *Chem. Commun.* **2005**, 4681–4683.
- [4] a) H. S. La Pierre, A. Scheurer, F. W. Heinemann, W. Hieringer, K. Meyer, *Angew. Chem. Int. Ed. Engl.* **2014**, *53*, 7158–7162; b) M. R. MacDonald, M. E. Fieser, J. E. Bates, J. W. Ziller, F. Furche, W. J. Evans, *J. Am. Chem. Soc.* **2013**, *135*, 13310–13313; c) F. S. Guo, N. Tsoureas, G. Z. Huang, M. L. Tong, A. Mansikkamaki, R. A. Layfield, *Angew. Chem. Int. Ed. Engl.* **2020**, *59*, 2299–2303; d) A. J. Ryan, M. A. Angadol, J. W. Ziller, W. J. Evans, *Chem. Commun.* **2019**, *55*, 2325–2327; e) D. N. Huh, J. W. Ziller, W. J. Evans, *Inorg. Chem.* **2018**, *57*, 11809–11814; f) D. N. Huh, C. J. Windorff, J. W. Ziller, W. J. Evans, *Chem. Commun.* **2018**, *54*, 10272–10275; g) B. S. Billow, B. N. Livesay, C. C. Mokhtarzadeh, J. McCracken, M. P. Shores, J. M. Boncella, A. L. Odom, *J. Am. Chem. Soc.* **2018**, *140*, 17369–17373.
- [5] a) S. A. Moehring, W. J. Evans, *Chem. Eur. J.* **2020**, *26*, 1530–1534; b) C. J. Windorff, M. R. MacDonald, K. R. Meihaus, J. W. Ziller, J. R. Long, W. J. Evans, *Chem. Eur. J.* **2016**, *22*, 772–782.
- [6] M. Falcone, L. Barluzzi, J. Andrez, F. F. Tirani, I. Zivkovic, A. Fabrizio, C. Corminboeuf, K. Severin, M. Mazzanti, *Nat. Chem.* **2019**, *11*, 154–160.
- [7] a) N. Jori, M. Falcone, R. Scopelliti, M. Mazzanti, *Organometallics* **2020**, *39*, 1590–1601; b) C. Camp, V. Mougél, J. Horeglad, J. Pecaut, M. Mazzanti, *J. Am. Chem. Soc.* **2010**, *132*, 17374–17377; c) J. J. Kiernicki, P. E. Fanwick, S. C. Bart, *Chem. Commun.* **2014**, *50*, 8189–8192; d) N. H. Anderson, S. O. Odoh, Y. Y. Yao, U. J. Williams, B. A. Schaefer, J. J. Kiernicki, A. J. Lewis, M. D. Goshert, P. E. Fanwick, E. J. Schelter, J. R. Walensky, L. Gagliardi, S. C. Bart, *Nat. Chem.* **2014**, *6*, 919–926; e) D. P. Cladis, J. J. Kiernicki, P. E. Fanwick, S. C. Bart, *Chem. Commun.* **2013**, *49*, 4169–4171; f) P. L. Diaconescu, P. L. Arnold, T. A. Baker, D. J. Mindiola, C. C. Cummins, *J. Am. Chem. Soc.* **2000**, *122*, 6108–6109.
- [8] L. Chatelain, R. Scopelliti, M. Mazzanti, *J. Am. Chem. Soc.* **2016**, *138*, 1784–1787.
- [9] B. Vlasisajjevich, P. L. Diaconescu, W. L. Lukens, Jr., L. Gagliardi, C. C. Cummins, *Organometallics* **2013**, *32*, 1341–1352.
- [10] P. L. Diaconescu, C. C. Cummins, *J. Chem. Soc.-Dalton Trans.* **2015**, *44*, 2676–2683.

RESEARCH ARTICLE

- [11] a) C. A. Gould, L. E. Darago, M. I. Gonzalez, S. Demir, J. R. Long, *Angew. Chem. Int. Ed. Engl.* **2017**, *56*, 10103-10107; b) S. Demir, M. Nippe, M. I. Gonzalez, J. R. Long, *Chem. Sci.* **2014**, *5*, 4701-4711; c) S. Demir, J. M. Zadrozny, M. Nippe, J. R. Long, *J. Am. Chem. Soc.* **2012**, *134*, 18546-18549.
- [12] a) L. Zhang, C. C. Zhang, G. H. Hou, G. F. Zi, M. D. Walter, *Organometallics* **2017**, *36*, 1179-1187; b) A. Mohammad, D. P. Cladis, W. P. Forrest, P. E. Fanwick, S. C. Bart, *Chem. Commun.* **2012**, *48*, 1671-1673; c) S. J. Kraft, P. E. Fanwick, S. C. Bart, *Inorg. Chem.* **2010**, *49*, 1103-1110; d) P. K. Yang, E. W. Zhou, B. Fang, G. H. Hou, G. F. Zi, M. D. Walter, *Organometallics* **2016**, *35*, 2129-2139.
- [13] a) W. J. Evans, D. K. Drummond, *J. Am. Chem. Soc.* **1989**, *111*, 3329-3335; b) G. Nocton, L. Ricard, *Chem. Commun.* **2015**, *51*, 3578-3581; c) G. Nocton, W. W. Lukens, C. H. Booth, S. S. Rozenel, S. A. Medling, L. Maron, R. A. Andersen, *J. Am. Chem. Soc.* **2014**, *136*, 8626-8641; d) W. J. Evans, G. W. Rabe, J. W. Ziller, *Inorg. Chem.* **1994**, *33*, 3072-3078; e) L. Maria, M. Soares, I. C. Santos, V. R. Sousa, E. Mora, J. Marcalo, K. V. Luzyanin, *J. Chem. Soc.-Dalton Trans.* **2016**, *45*, 3778-3790; f) S. Labouille, F. Nief, X. F. Le Goff, L. Maron, D. R. Kindra, H. L. Houghton, J. W. Ziller, W. J. Evans, *Organometallics* **2012**, *31*, 5196-5203.
- [14] a) F. Jaroschik, F. Nief, X. F. Le Goff, L. Ricard, *Organometallics* **2007**, *26*, 3552-3558; b) I. L. Fedushkin, V. I. Nevodchikov, M. N. Bochkarev, S. Dechert, H. Schumann, *Russ. Chem. Bull.* **2003**, *52*, 154-159.
- [15] A. Formanuk, F. Ortu, J. J. Liu, L. E. Nodarak, F. Tuna, A. Kerridge, D. P. Mills, *Chem. Eur. J.* **2017**, *23*, 2290-2293.
- [16] a) T. Mehdoui, J. C. Berthet, P. Thuery, M. Ephritikhine, *Eur. J. Inorg. Chem.* **2004**, 1996-2000; b) J. C. Berthet, P. Thuery, C. Baudin, B. Boizot, M. Ephritikhine, *J. Chem. Soc.-Dalton Trans.* **2009**, 7613-7616.
- [17] a) T. Mehdoui, J. C. Berthet, P. Thuery, M. Ephritikhine, **2013**; b) T. Mehdoui, J. C. Berthet, P. Thuery, M. Ephritikhine, *J. Chem. Soc.-Dalton Trans.* **2004**, 579-590.
- [18] M. W. Rosenzweig, F. W. Heinemann, L. Maron, K. Meyer, *Inorg. Chem.* **2017**, *56*, 2792-2800.
- [19] a) M. K. Takase, M. Fang, J. W. Ziller, F. Furche, W. J. Evans, *Inorg. Chim. Acta* **2010**, *364*, 167-171; b) G. F. Zi, L. Jia, E. L. Werkema, M. D. Walter, J. P. Gottfriedsen, R. A. Andersen, *Organometallics* **2005**, *24*, 4251-4264; c) T. Mehdoui, J. C. Berthet, P. Thuery, L. Salmon, E. Riviere, M. Ephritikhine, *Chem. Eur. J.* **2005**, *11*, 6994-7006.
- [20] S. Fortier, J. Veleta, A. Pialat, J. Le Roy, K. B. Ghiassi, M. M. Olmstead, A. Metta-Magana, M. Murugesu, D. Villagran, *Chem. Eur. J.* **2016**, *22*, 1931-1936.
- [21] J. X. Wang, Y. Gurevich, M. Botoshansky, M. S. Eisen, *J. Am. Chem. Soc.* **2006**, *128*, 9350-9351.
- [22] a) O. P. Lam, S. C. Bart, H. Kameo, F. W. Heinemann, K. Meyer, *Chem. Commun.* **2010**, *46*, 3137-3139; b) L. Castro, O. P. Lam, S. C. Bart, K. Meyer, L. Maron, *Organometallics* **2010**, *29*, 5504-5510; c) S. Fortier, J. L. Brown, N. Kaltsoyannis, G. Wu, T. W. Hayton, *Inorg. Chem.* **2012**, *51*, 1625-1633; d) J. C. Berthet, M. Lance, M. Nierlich, J. Vigner, M. Ephritikhine, *J. Organomet. Chem.* **1991**, *420*, C9-C11; e) A. C. Schmidt, A. V. Nizovtsev, A. Scheurer, F. W. Heinemann, K. Meyer, *Chem. Commun.* **2012**, *48*, 8634-8636; f) A. S. P. Frey, F. G. N. Cloke, M. P. Coles, P. B. Hitchcock, *Chem. Eur. J.* **2010**, *16*, 9446-9448.
- [23] W. J. Evans, S. A. Kozimor, J. W. Ziller, *Polyhedron* **2004**, *23*, 2689-2694.
- [24] B. E. Cowie, I. Douair, M. Laurent, J. B. Love, P. L. Arnold, *Chem. Sci.* **2020**, *11*, 7144-7157.
- [25] a) J. Rosenthal, T. D. Luckett, J. M. Hodgkiss, D. G. Nocera, *J. Am. Chem. Soc.* **2006**, *128*, 6546-6547; b) J. Rosenthal, J. Bachman, J. L. Dempsey, A. J. Esswein, T. G. Gray, J. M. Hodgkiss, D. R. Manke, T. D. Luckett, B. J. Pistorio, A. S. Veige, D. G. Nocera, *Coord. Chem. Rev.* **2005**, *249*, 1316-1326.
- [26] B. J. Tabner, J. R. Yandle, *Journal of the Chemical Society a -Inorganic Physical Theoretical* **1968**, 381-8.
- [27] a) T. R. Dugan, E. Bill, K. C. MacLeod, G. J. Christian, R. E. Cowley, W. W. Brennessel, S. Ye, F. Neese, P. L. Holland, *J. Am. Chem. Soc.* **2012**, *134*, 20352-20364; b) C. T. Carver, P. L. Diaconescu, *J. Am. Chem. Soc.* **2008**, *130*, 7558-7559; c) B. R. Cockerton, A. J. Deeming, *J. Organomet. Chem.* **1992**, *426*, C36-C39; d) H. S. Soo, P. L. Diaconescu, C. C. Cummins, *Organometallics* **2004**, *23*, 498-503.
- [28] W. L. Huang, S. I. Khan, P. L. Diaconescu, *J. Am. Chem. Soc.* **2011**, *133*, 10410-10413.
- [29] I. Korobkov, S. Gambarotta, G. P. A. Yap, *Angew. Chem. Int. Ed. Engl.* **2002**, *41*, 3433-3436.
- [30] M. H. Chisholm, J. C. Huffman, I. P. Rothwell, P. G. Bradley, N. Kress, W. H. Woodruff, *J. Am. Chem. Soc.* **1981**, *103*, 4945-4947.
- [31] A. J. Lewis, U. J. Williams, P. J. Carroll, E. J. Schelter, *Inorg. Chem.* **2013**, *52*, 7326-7328.
- [32] M. Irwin, T. Kramer, J. E. McGrady, J. M. Goicoechea, *Inorg. Chem.* **2011**, *50*, 5006-5014.
- [33] J. C. Berthet, P. Thuery, N. Garin, J. P. Dognon, T. Cantat, M. Ephritikhine, *J. Am. Chem. Soc.* **2013**, *135*, 10003-10006.
- [34] W. S. Ren, G. F. Zi, M. D. Walter, *Organometallics* **2012**, *31*, 672-679.
- [35] T. R. Dugan, E. Bill, K. C. MacLeod, G. J. Christian, R. E. Cowley, W. W. Brennessel, S. F. Ye, F. Neese, P. L. Holland, *J. Am. Chem. Soc.* **2012**, *134*, 20352-20364.

Entry for the Table of Contents



A molecular diuranium(III) oxide was prepared and its molecular and electronic structure were determined by crystallographic and computational studies. The complex undergoes cleavage of one U-O bonding and effects the reductive coupling of pyridine and the two-electron reduction of bipyridine by delivering a "U(II)" synthon. These reactions provide a synthetic route to dinuclear U(III)/U(III) complexes bridged by redox-active N-heterocyclic ligands.

Twitter usernames: [@mazzantilab](#)